Ab Initio Study of Hydrogen Bonding in the Phenol–Water System

David Feller*[1] and Martin W. Feyereisen[2]

[1]Theory, Modeling, and Simulation, Molecular Science Research Center, Pacific Northwest Laboratory,† Richland, Washington 99352, and [2]CRAY Research, Inc., Eagan, Minnesota 55121

Three hydrogen-bonded minima on the phenol–water, C_6H_5OH—H_2O, potential energy surface were located with 3-21G and 6-31G** basis sets at both Hartree–Fock and MP2 levels of theory. MP2 binding energies were computed using large "correlation consistent" basis sets that included extra diffuse functions on all atoms. An estimate of the effect of expanding the basis set to the triple-zeta level (multiple f functions on carbon and oxygen and multiple d functions on hydrogen) was derived from calculations on a related prototype system. The best estimates of the electronic binding energies for the three minima are -7.8, -5.0, and -2.0 kcal/mol. The consequences of uncertainties in the geometries and limitations in the level of correlation recovery are analyzed. It is suggested that our best estimates will likely underestimate the complete basis set, full CI values by 0.1–0.3 kcal/mol. Vibrational normal modes were determined for all three minima, including an MP2/6-31G** analysis for the most strongly bound complex. Computational strategies for larger phenol–water complexes are discussed. © 1993 by John Wiley & Sons, Inc.

INTRODUCTION

Phenol is representative of a class of aromatic alcohols present as soil contaminants at nuclear materials processing sites, including the U.S. Department of Energy's Hanford Reservation. While a large number of potential chemical interactions are pertinent to an understanding of the Hanford aquifers, clearly those involving water assume an added importance. Because techniques to model fundamental chemical processes in solution are a primary goal of the Molecular Science Research Center at Pacific Northwest Laboratory, we have begun an *ab initio* study of small phenol–water complexes as a prelude to carrying out molecular dynamics simulations of these and larger systems.

A vital first step in understanding the weak solute–solvent interaction energy in molecular systems containing more than a dozen atoms is the identification of a balanced level of theory that is computationally tractable yet sufficiently accurate to measure bond strengths of less than 10 kcal/mol. Extended basis sets and highly correlated *ab initio* methods are still too time consuming to be directly applied to large molecular clusters, even on today's fastest computers. Nonetheless, high-accuracy, quantum chemical structures and binding energies are important to help improve the faster but more approximate methods that are being used on larger systems. Results of the present study will be used in support of recently proposed nonadditive intermolecular potentials.[1,2]

In this work, we focus on identifying potential sites for hydrogen bond formation between the phenol ring and a single water molecule to calibrate our methods. A previous study[3] of the H_2O—H_2O binding energy using extensive basis sets and correlation recovery found that a relatively modest level of theory was sufficient to obtain results within ~ 1 kcal/mol. Hartree–Fock (HF) theory is capable of accounting for most of the attractive forces operating between closed-shell, hydrogen-bonded fragments. A limited amount of correlation recovery, such as through second-order Møller–Plesset perturbation theory (MP2), accounts for most of the remainder of the interaction energy. Increased correlation recovery through fourth-order perturbation (MP4) theory or quadratic configuration interaction (QCISD)[4] changed the binding energy by no more than 0.1–0.2 kcal/mol.

There have been no published experimental reports of the phenol–water binding energy. Despite this, recent experimental developments such as the cluster ion dip technique of Stanley and Castleman[5] and the work of Ebata et al.[6] provided information about some low-frequency intermolecular vibrational modes in small phenol–water clusters. These results provide some insight as to the accuracy of the present calculations.

---

*Author to whom all correspondence should be addressed.

†The Pacific Northwest Laboratory is operated for the U.S. Department of Energy by Battelle Memorial Institute under Contract DE-AC06-76RLO 1830.

As this article was nearing completion, we became aware of other recent theoretical work on phenol–water. Schütz et al.[7] performed 4-31G and 6-31G** HF geometry optimization and vibrational normal mode analysis for a single water interacting with phenol. No attempt was made to correct the results for basis set superposition errors (BSSE) or for correlation effects. Thus, because we tended to focus on the use of larger basis sets and correlated methods our two studies offer complementary approaches to the same subject. The characterization of the phenol and phenol–water normal modes at a higher level of theory, as presented in the current work, should facilitate the task of assigning the observed bands and help answer the computational question concerning the need for correlated methods in determining vibrational frequencies.

PROCEDURE

Minima on the phenol–water potential energy surface were identified by means of HF and MP2 calculations employing valence double-zeta (3-21G)[8] and valence double-zeta + polarization (6-31G**)[9] basis sets. For the complex, these two sets resulted in 88 and 160 basis functions, respectively. The three methods (HF/3-21G, HF/6-31G**, and MP2/6-31G**) span more than two orders of magnitude in computational cost.

Calculations on the water dimer by Frisch et al.[10] showed the O—O distance in $(H_2O)_2$ to be more than 0.1 Å shorter at the HF/3-21G level than the value predicted by extended basis set MP2 calculations and almost 0.18 Å shorter than experiment. The addition of polarization functions on all atoms improves this situation. For example, the MP2/6-31G** O—O distance was within 0.001 Å of the apparent basis set limit. The single exception is the angle between the bisector of the HOH angle on the proton acceptor fragment and a line connecting the two oxygens, which Frisch et al.[10] labeled "Θ_a." This angle remains *underestimated* at the MP2/6-31G** level by over 20°. An even larger basis set, such as 6-31++G**,[11] would have reduced the size of the error in Θ_a but would have been prohibitively large for performing MP2 normal mode analyses. All geometry optimizations were performed with the Gaussian 90 program.[12]

Once the minima were identified at the MP2/6-31G** level, larger basis set correlated calculations were performed with DISCO,[13] a direct SCF/MP2 program, to more accurately determine the binding energies. Most of these calculations were performed with the cc-pVDZ correlation consistent basis set[14] and its diffuse-function-augmented counterpart (aug-cc-pVDZ).[15] The latter is a $[4s,3p,2d/3s,2p]$ contraction of a $(10s,5p,2d/5s,2p)$ Gaussian primitive set. It produced a total of 256 functions when
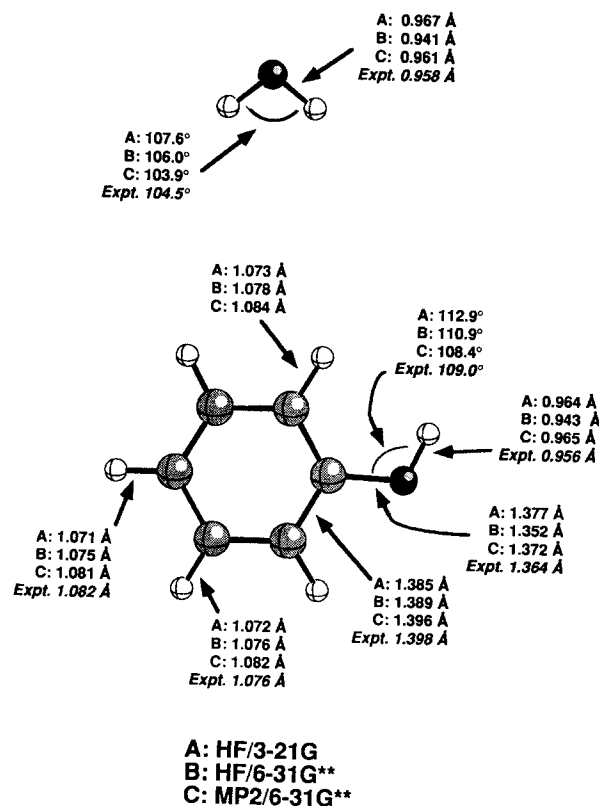
applied to the phenol–water complex. Calculations employing the aug-cc-pVTZ set, a $[5s,4p,3d,2f/ 4s,3p,2d]$ contraction, were carried out on a prototype of the phenol–water system.
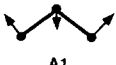
RESULTS

Geometries and Vibrational Frequencies

In Figure 1, the geometries of the isolated water and phenol molecules obtained at the three levels of theory mentioned above are displayed along with the available experimental data.[16,17] As is evident, both fragments are well described with even modest levels of theory. Although the MP2/6-31G** results exhibit the best overall agreement with experiment,[18] the differences with respect to the other two levels of theory are not great. The largest spread in bond lengths is less than 0.02 Å and in bond angles less than 4°, a situation typical of the performance of these methods on other first- and second-period closed-shell compounds.[19]

Harmonic vibrational frequencies for the two molecules are shown in Figures 2 and 3 along with experimental frequencies.[20–22] HF/3-21G frequencies are not shown for phenol but are in general within 10% of the HF/6-31G** values. The largest differences were observed for the high-frequency stretch-
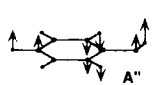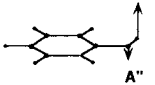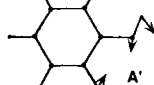

A: 0.967 Å
B: 0.941 Å
C: 0.961 Å
Expt. 0.958 Å

A: 107.6°
B: 106.0°
C: 103.9°
Expt. 104.5°

A: 1.073 Å
B: 1.078 Å
C: 1.084 Å

A: 112.9°
B: 110.9°
C: 108.4°
Expt. 109.0°

A: 0.964 Å
B: 0.943 Å
C: 0.965 Å
Expt. 0.956 Å

A: 1.377 Å
B: 1.352 Å
C: 1.372 Å
Expt. 1.364 Å

A: 1.071 Å
B: 1.075 Å
C: 1.081 Å
Expt. 1.082 Å

A: 1.385 Å
B: 1.389 Å
C: 1.396 Å
Expt. 1.398 Å

A: 1.072 Å
B: 1.076 Å
C: 1.082 Å
Expt. 1.076 Å

A: HF/3-21G
B: HF/6-31G**
C: MP2/6-31G**
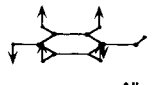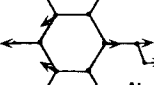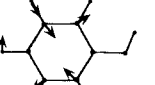
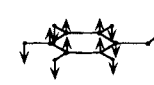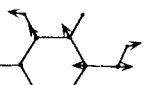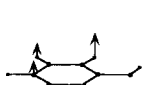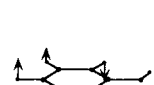**Figure 1.** Water- and phenol-optimized geometries and the available experimental values.

	A1	A1	B2
3-21G/HF	1799.3	3812.4	3945.8
6-31G**/HF	1769.6	4147.6	4264.6
6-31G**/HF (scaled)	1580.3	3703.8	3808.3
6-31G**/MP2	1683.5	3894.5	4033.2
Expt.	1595	3657	3756
Expt. (harmonic)	1648	3832	3943
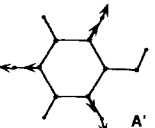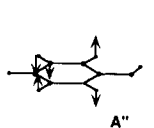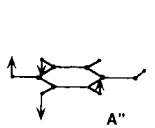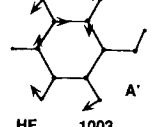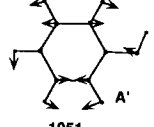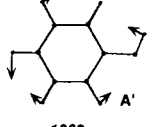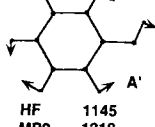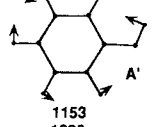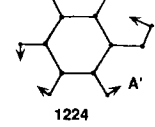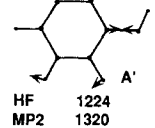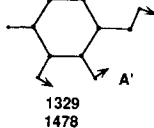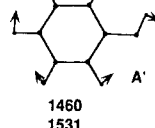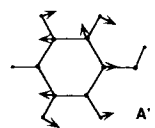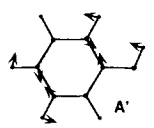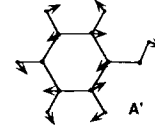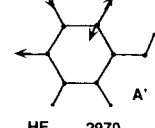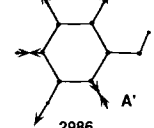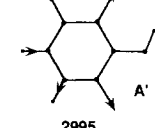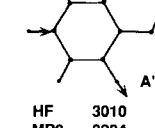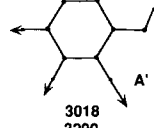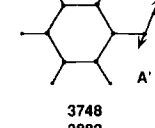
Figure 2. Harmonic theoretical vibrational frequencies (cm⁻¹) for the water molecule and the available experimental values.

ing modes, with low-frequency bends in general being within 3% of the value obtained at the two higher levels of theory. For example, the bending mode in water is predicted to have a frequency of 1799 cm⁻¹ (HF/3-21G) and 1770 cm⁻¹ (HF/6-31G**), while the lowest out-of-plane bend in phenol is 265 cm⁻¹ (HF/3-21G) and 256 cm⁻¹ (HF/6-31G**).

A scale factor of 0.893 has been applied to the computed HF/6-31G** values to improve agreement with experiment, as suggested by Pople et al.[23] Schütz et al.[7] found that the optimal scale value for phenol at the HF/6-31G** level of theory was slightly larger (0.9028). The MP2 frequencies in Figure 3 have

HF	229	280	394
MP2	227	327	403
Expt	244	309	404, 408

HF	442	507	512
MP2	405	465	522
Expt	410	503	527, 527

HF	606	686	756
MP2	535	633	736
Expt	619, 619	687	752

HF	797	825	889
MP2	814	837	850
Expt	823, 823	817	881

Figure 3. Harmonic theoretical (HF/6-31G** and MP2/6-31G**) vibrational frequencies (cm⁻¹) for the phenol molecule and the available experimental values. The HF values have been scaled by 0.893. When two values are given the first is taken from ref. 19 and the second from ref. 18.

HF	960	973	993
MP2	905	913	1024
Expt	1000, 999	973	995

HF	1003	1051	1069
MP2	1064	1117	1205
Expt	1026, 1026	1070, 1072	1177, 1169

HF	1145	1153	1224
MP2	1218	1220	1321
Expt	1150, 1261	1169	1343

HF	1224	1329	1460
MP2	1320	1478	1531
Expt	1262	1277	1472

HF	1492	1606	1617
MP2	1567	1681	1695
Expt	1502	1610	1604

HF	2970	2986	2995
MP2	3242	3262	3270
Expt	3027	3049	3063

HF	3010	3018	3748
MP2	3284	3290	3882
Expt	3070	3087	3656

Figure 3. (continued)

not been scaled. The rms deviations with respect to experimental values for phenol and water are 76 cm⁻¹ (scaled HF/3-21G), 44 cm⁻¹ (scaled HF/6-31G**), 56 cm⁻¹, and 123 cm⁻¹ (scale = 0.94 and unscaled MP2/6-31G**). While the scaled HF/6-31G** frequencies exhibit a somewhat smaller rms error than the scaled MP2 results, the principal improvement resulting from correlation recovery is a large decrease in the error in the unscaled frequencies, which drops from 214 to 105 cm⁻¹. The deviation with respect to the limited experimental data

for the complex was sufficiently small that ΔE_{ZPE} should be able to be estimated to within 1.0 kcal/mol.

Four potential sites for hydrogen bonding were examined. One of these, in which a water molecule was situated above the center of the phenol ring, displayed a minimum at the HF/3-21G level, but all attempts to locate a similar 6-31G** minimum failed. When optimization runs were started in the "above ring" position, the system slowly converged to one of the structures displayed in Figure 4, which shows the two lowest-energy forms of the complex. In the top structure, designated conformation (1), water serves as a proton acceptor. In the second structure, referred to as conformation (2), water acts as a proton donor to the phenol oxygen. Selected internuclear distances and bond angles obtained from the three levels of theory discussed previously are given.

Several of the lower-frequency modes of confirmation (1) are shown in Figure 5. The hydrogen bond stretching mode, which gives rise to an intense fluorescence band at 150 cm^{-1}, is well described by these calculations. It is bounded by the 6-31G** HF and MP2 values. The corresponding scaled HF/3-21G frequency is 193 cm^{-1}, somewhat larger than either experimental value or the other two theoretical values. A lower-frequency wag, estimated by Schütz et al.[7] at 69 cm^{-1} using half the overtone frequency, is likewise well reproduced.
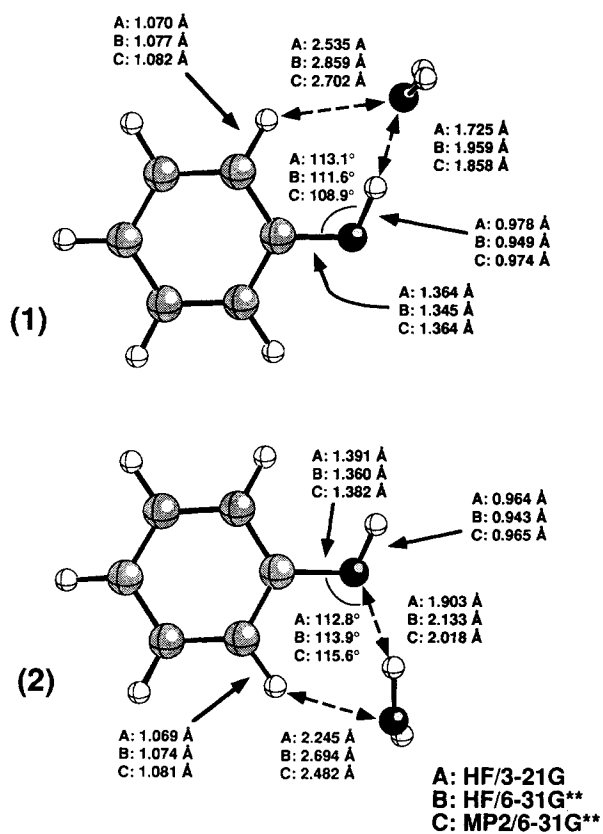
Figure 4. Optimized phenol–water hydrogen-bonded structures for the two lowest-energy complexes.
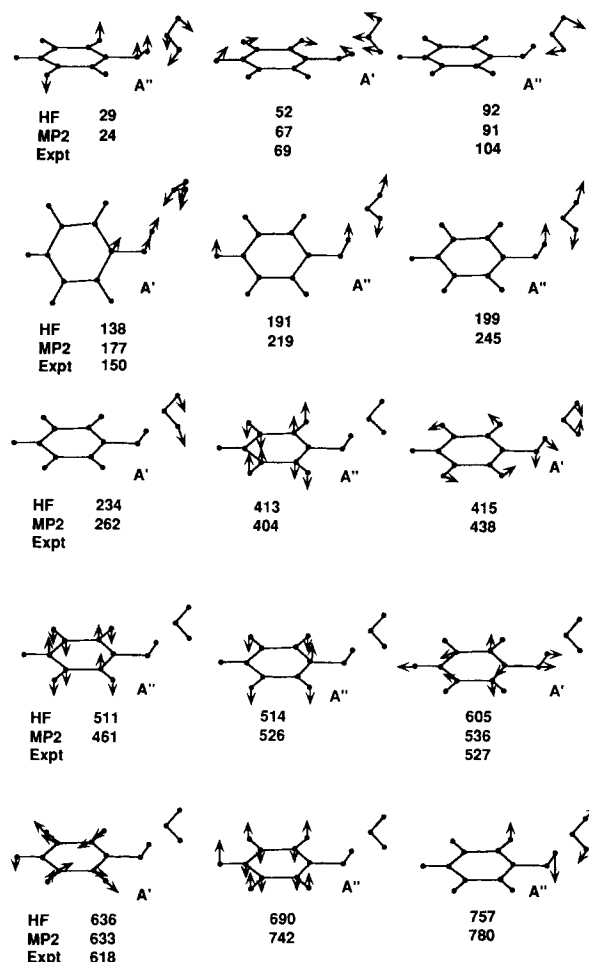
Figure 5. Selected phenol–water harmonic (HF/6-31G** and MP2/6-31G**) vibrational frequencies (cm^{-1}) and the available experimental values, taken from Ebata et al.[7] The experimental frequency for the lowest a' mode was estimated as half the overtone frequency by Schütz et al.[8]

Theory has a difficult time estimating the small, subtle changes in frequency that accompany hydrogen bond formation. For example, in the water dimer one of the HOH bends decreases by 2 cm^{-1}, while the other increases by 16 cm^{-1} relative to the value in the isolate water molecule. Likewise, one of the symmetric stretches decreases by 30 cm^{-1} and the other by 57 cm^{-1}. MP2 calculations typically are in error by 50%. For geometry (1), there is one relatively large change in frequency, as noted by Schütz et al.,[7] which involves a torsional motion of the OH group. This mode in phenol is the second lowest frequency mode of a'' symmetry (327 cm^{-1} MP2) in Figure 3 and in phenol–water is the highest a'' mode shown in Figure 5 (780 cm^{-1} MP2). This 453 cm^{-1} change represents a 138% increase over the phenol value. It is the result of a coupling between the torsional motion and an asymmetric stretching motion in the water molecule.

A third minimum, labeled (3) in Figure 6, was also identified at the same levels of theory used for structures (1) and (2). This minimum, characterized by a

(3)

A: 1.072 Å
B: 1.075 Å
C: 1.081 Å

A: 2.227 Å
B: 2.577 Å
C: 2.440 Å

A: 102.6°
B: 109.0°
C: 109.3°

A: HF/3-21G
B: HF/6-31G**
C: MP2/6-31G**

A: 0.964Å
B: 0.942 Å
C: 0.965 Å

A: 1.379 Å
B: 1.353 Å
C: 1.375 Å

A: 1.074 Å
B: 1.076 Å
C: 1.081 Å

A: 2.248 Å
B: 2.573 Å
C: 2.379 Å

(Transition State)
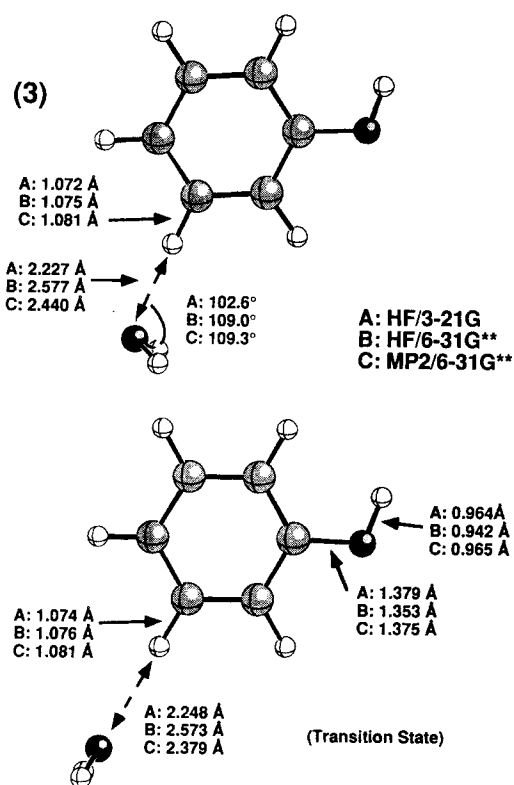
Figure 6. Optimized phenol–water hydrogen-bonded conformation with the smallest binding energy.

hydrogen bond to a hydrogen in the meta ring position, is representative of related conformations involving hydrogen bonds in the para and other meta positions. However, no explicit search for the other

potential minima was performed. All attempts to identify an ortho minimum were unsuccessful, as the optimizations invariably collapsed to conformation (1) or (2). The transition state for flipping the water molecule about the hydrogen bond is also shown in Figure 6. As might be expected from the elongated hydrogen bond, the water molecule is only loosely bound and insensitive to its orientation with respect to the phenol ring. Thus, the transition state is a mere 0.5 kcal/mol higher in energy than the minimum.

Compared with the O—O distance in the water dimer, the O—O distance in conformation (1) is predicted to be shorter by between 0.097 Å (HF/3-21G) and 0.081 Å (MP2/6-31G**), suggesting that the phenol–water hydrogen bond is substantially stronger. Conversely, for (2) the O—O distance is predicted to be 2.94 Å (MP2/6-31G**) or about 0.03 Å longer than in the water dimer, suggesting a slightly weaker bond. Finally, in (3) the phenol (H)—OH_2 distance assumes a value of 2.38 Å compared to 1.95 Å in $(H_2O)_2$, reflecting its weak hydrogen bond.

Binding Energies

Electronic binding energies for all three conformations are listed in Table I at optimal geometries determined by various combinations of the basis sets and levels of theory previously discussed. The corresponding total energies are given in Table II. MP2 results for the correlation consistent basis sets were obtained within the frozen core approximation. Be-

Table I. Phenol–water hydrogen bond strengths.

Basis Set	Method	Geometry	$\Delta E_{binding}$	ΔE (CP)[a]
Structure 1				
3-21G	HF	HF/3-21G	−15.4	−9.4
6-31G**	HF	HF/6-31G**	−7.3	−6.2
	MP2	MP2/6-31G**	−9.5	−6.9
cc-pVDZ	HF	MP2/6-31G**	−7.8	−5.9
	MP2(FC)	MP2/6-31G**	−10.9	−6.1
aug-cc-pVDZ	HF	HF/3-21G	−3.5	−3.4
	MP2(FC)	HF/3-21G	−6.8	
	HF	MP2/6-31G**	−4.7	−4.6
	MP2(FC)	MP2/6-31G**	−7.7	−6.2
	MP2(FC)	(MP2/6-31++G**)[b]	−8.0	−6.5
est. aug-cc-pVTZ	MP2(FC)	MP2/6-31G**	−7.5	−6.6
Structure 2				
3-21G	HF	HF/3-21G	−11.5	−3.8
6-31G**	HF	HF/6-31G**	−4.7	−3.5
	MP2	MP2/6-31G**	−7.1	−3.5
aug-cc-pVDZ	HF	MP2/6-31G**	−2.1	−2.0
	MP2(FC)	MP2/6-31G**	−5.0	−3.6
	MP2(FC)	(MP2/6-31++G**)[b]	−5.2	−3.8
Structure 3				
3-21G	HF	HF/3-21G	−5.5	−0.8
6-31G**	HF	HF/6-31G**	−1.8	−0.6
	MP2	MP2/6-31G**	−2.7	−0.7
aug-cc-pVDZ	HF	MP2/6-31G**	−0.5	−0.4
	MP2(FC)	MP2/6-31G**	−2.0	−1.1

Binding energies are given in kcal/mol. Entries labeled MP2(FC) were obtained from frozen core calculations.
[a]Counterpoise-corrected binding energy.
[b]Partial reoptimization with diffuse functions added to water and one of the phenol ring hydrogens.

Table II. Phenol–water total energies.

Basis Set	Method	Geometry	Energy
Structure 1			
3-21G	HF	HF/3-21G	−379.4706
6-31G**	HF	HF/6-31G**	−381.6089
	MP2	MP2/6-31G**	−382.8131
cc-pVDZ	HF	MP2/6-31G**	−381.6260
	MP2(FC)	MP2/6-31G**	−382.7990
aug-cc-pVDZ	HF	HF/3-21G	−381.6501
	MP2(FC)	HF/3-21G	−382.8823
	HF	MP2/6-31G**	−381.6490
	MP2(FC)	MP2/6-31G**	−382.8830
	MP2(FC)	(MP2/6-31++G**)[a]	−382.8832
Structure 2			
3-21G	HF	HF/3-21G	−379.4645
6-31G**	HF	HF/6-31G**	−381.6048
	MP2	MP2/6-31G**	−382.8092
aug-cc-pVDZ	HF	MP2/6-31G**	−381.6459
	MP2(FC)	MP2/6-31G**	−382.8780
	MP2(FC)	(MP2/6-31++G**)[a]	−382.8783
Structure 3			
3-21G	HF	HF/3-21G	−379.4549
6-31G**	HF	HF/6-31G**	−381.6002
	MP2	MP2/6-31G**	−382.8023
aug-cc-pVDZ	HF	MP2/6-31G**	−381.6434
	MP2(FC)	MP2/6-31G**	−382.8731

Energies given in Hartrees.
[a]Partial reoptimization with diffuse functions added to water and one of the phenol hydrogens.

cause hydrogen bond strengths are typically on the order of 5 kcal/mol or less, it is important to take into account the so-called BSSE when computing $\Delta E_{binding}$. This error arises from the use of finite basis sets and produces an intrafragment energy lowering that masquerades as interfragment binding energy. When molecular fragments approach each other, they can lower their own energy by exploiting basis functions on neighboring centers. With certain basis sets and levels of theory, the BSSE can more than double the estimate of the binding energy. As the basis set on each fragment approaches completeness, the BSSE tends to zero.

We have chosen to use the function counterpoise (CP) method first suggested by Boys and Bernardi[24] to estimate the size of the BSSE contribution. The findings of the water dimer study[3] demonstrated that application of the CP correction substantially *improved* agreement between results obtained from diffuse-function-deficient basis sets and the apparent complete basis set limit but *worsened* agreement for other sets. Thus, we shall apply the method with reservation. To the extent that the water dimer results apply in this case, the CP-corrected *aug*-cc-pVxZ results will underestimate the true binding energy.

In Table I, the size of the CP *correction* to the $\Delta E_{binding}$ of conformation (1) ranges from +6.0 kcal/mol at the HF/3-21G level to +0.9 kcal/mol at the estimated MP2/aug-cc-pVTZ level. The 6-31G** or cc-pVDZ MP2 entries in Table I exhibit corrections in the 3- to 4-kcal/mol range. With the addition of an extra shell of diffuse functions, the aug-cc-pVDZ CP-corrected binding energies differ by no more than

0.1 and 1.6 kcal/mol from their uncorrected HF and MP2 counterparts, respectively. In the case of the water dimer, it was necessary to resort to basis sets of the aug-cc-pVTZ type to reduce the magnitude of CP correction to less than 1 kcal/mol.

Of the three main factors affecting the reliability of the computed $\Delta E_{binding}$ (basis set quality, accuracy in the geometry, and level of theory), Table I addresses the first two. To gauge the convergence of the phenol–water binding energy with respect to the completeness of the basis set, it would have been instructive to perform the same sequence of aug-cc-pVDZ, aug-cc-pVTZ, and aug-cc-pVQZ MP2 calculations as were done for the water dimer study. In that case, the aug-cc-pVDZ binding energy differed by just 0.1 kcal/mol from the aug-cc-pVQZ value,[3] even though the number of basis functions differed by more than 250. However, for phenol–water the next larger basis set (aug-cc-pVTZ) would have necessitated a 550-function MP2 calculation. As it was, the 256-function, aug-cc-pVDZ calculations were taking 0.6–1.4 CPU h/SCF iteration and between 4.7–10.1 CPU h for a fully direct MP2 energy evaluation running on a high-speed workstation. We chose instead to model a portion of the phenol ring with ethanol (constrained to have the same geometry), as indicated in Figure 7. Even with the replacement of the phenol ring by the frozen-geometry ethanol fragment the aug-cc-pVTZ basis set, which was the largest set used in the present study, resulted in a total of 368 functions. The resulting MP2 calculations required approximately 20 CPU h on a CRAY 2.

Mulliken charges on the two ethanol hydrogens
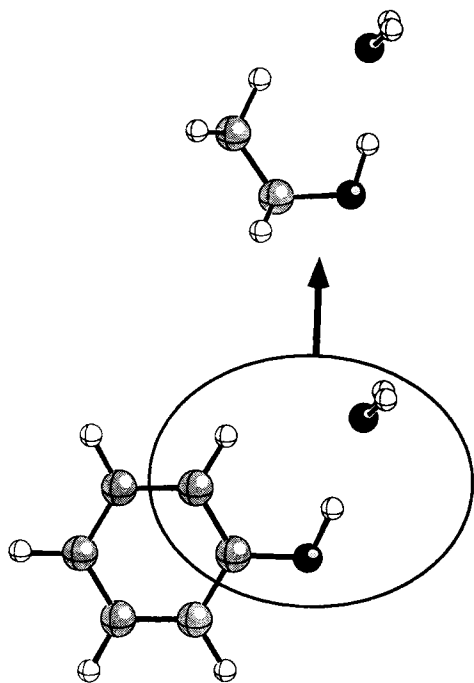
Figure 7. Ethanol–water fragment used for the MP2/aug-cc-pVTZ basis calculations.

oriented toward the water molecule were nearly identical to their values in the phenol ring [e.g., +0.39 (phenol hydroxy H) vs. +0.37 (ethanol H)], suggesting that constrained ethanol should serve as a reasonable model for the ring. A comparison of the aug-cc-pVDZ binding energies shows ethanol–water to have a 2-kcal/mol weaker bond than phenol–water, so the prototype is not a perfect substitute for the larger system. However, it did allow us to test the effects of the larger triple-zeta basis. The binding energy was found to be only slightly (0.2 kcal/mol) larger. CP corrections were within 0.1 kcal/mol for the two systems. The entry labeled "est. aug-cc-pVTZ" in Table I assumes the transferability of the +0.2-kcal/mol triple-zeta correction to the binding energy from the ethanol–water system to the phenol–water system.

While small, the effect on the binding energy of increasing the basis set to the aug-cc-pVTZ level was roughly twice what was observed in the water dimer. The effect of the CP correction was also larger, *increasing* $\Delta E_{\mathrm{binding}}$ by 0.5 kcal/mol vs. 0.3 for $(H_2O)_2$. This increased sensitivity to the basis set may reflect the fact that in (1) and (2) the phenol ring presents water with two positions where its basis functions can extend onto the other fragment.

As was true in the case of the water dimer, the CP-corrected binding energy changed by a greater amount than the uncorrected result. Because of this, it was concluded that the correction does not work well with basis sets containing diffuse functions. Del Bene reached[25] similar conclusions based on cal-

culations on $(HF)_2$, $(H_2O)_2$, and FH $\cdots$ NCH. Thus, our best estimate of the binding energy of conformation (1) uses the est. aug-cc-pVTZ value of -7.5 kcal/mol at the optimal MP2/6-31G** geometry and adds an estimated -0.3-kcal/mol correction that results from reoptimization at the MP2/6-31+ +G** level. We have not carried out similar ethanol–water prototype calculations for geometry (2). To the extent the bonding in (2) follows a similar trend, the $\Delta E_{\mathrm{binding}}$ basis set limit at the MP2/6-31G** geometry is estimated to be -4.8 kcal/mol.

An additional 0.2- to 0.3-kcal/mol increase to the binding energy was found from partial reoptimization of the geometry of the position of the water molecule with respect to the ring using a basis set containing diffuse (sp/s) Gaussian primitives on water and the phenol hydrogen involved in the hydrogen bond. At the MP2 level, this 167-function basis set predicts somewhat longer hydrogen bonds (~ 0.025 Å) compared to the 6-31G** value. The OH bonds in H_2O are also slightly lengthened, but the effect on the fragment's energy is much less, resulting in the net increase in binding energy. This effect largely cancels the +0.2-kcal/mol decrease in binding energy from going to the aug-cc-pVTZ basis set. By combining the effects of the revised geometries and the triple-zeta basis set, we arrive at final electronic binding energies of -7.8 and -5.0 kcal/mol for conformations (1) and (2), respectively.

It is likely that improvements in the basis set used to determine the geometries of these hydrogen-bonded complexes, such as the addition of diffuse functions on all atoms or the inclusion of extra polarization functions, would result in small increases (~ 0.1–0.3 kcal/mol) in the computed binding energies but at an enormous expense in computer resources. Based on MP4 and QCISD(T) results for the water dimer, the current estimates of $\Delta E_{\mathrm{binding}}$ probably approach the full CI result from below.

Schütz et al.[7] calculated the D_e binding energy of (1) to be -7.3 kcal/mol based on HF/6-31G** calculations that were not corrected for BSSE effects. The authors state that "... the overestimate due to BSSE and the underestimate due to lack of electron correlation may fortuitously cancel rather closely." Our own 6-31G** MP2 CP-corrected results show a net +0.4-kcal/mol contribution to the binding energy from the sum of these opposing effects. Our own final estimate of D_e, which includes (1) the effects of significantly increasing the size of the basis set, (2) geometry reoptimization at a better level of theory, and (3) use of correlated methods for computing energies, found a value that was, in the end, only 0.5 kcal/mol larger than their raw HF/6-31G** result. Similarly for structure (2), the raw HF/6-31G** binding energy is only 0.3 kcal/mol less than the large basis set, correlated estimate. However, despite the close agreement of these results, methods that attempt to compute bond energies of ≤ 8 kcal/

Table III. Enthalpy adjustments to the electronic binding energy (kcal/mol).

	ΔE^0_{ZPE}	$\Delta(\Delta E_{ZPE})^{298}$	ΔE^{298}_{rot}	ΔE^{298}_{trans}	ΔPV	Total
Structure 1						
HF/3-21G	2.24	2.05	-0.89	-0.89	-0.59	1.92
HF/6-31G**	1.51	2.36	-0.89	-0.89	-0.59	1.50
MP2/6-31G**	1.82	2.28	-0.89	-0.89	-0.59	1.73
Structure 2						
HF/3-21G	2.51	1.84	-0.89	-0.89	-0.59	1.98
HF/6-31G**	1.53	2.31	-0.89	-0.89	-0.59	1.47
Structure 3						
HF/3-21G	1.36	2.59	-0.89	-0.89	-0.59	1.58
HF/6-31G**	0.63	2.93	-0.89	-0.89	-0.59	1.19

HF vibrational frequencies were scaled by 0.893. The change in zero point energy as a function of temperature was computed from the expression $RT[\Sigma_i(\nu_i/e^{u}i - 1) - \Sigma_j(\nu_j/e^{u}j - 1)]$, where the summations over i and j correspond to the isolated water and phenol and the bonded complex, respectively.

mol and fail to include effects that amount to 2–3 kcal/mol should be used with caution.

Based on the data in Table I, structure (3) is clearly the least strongly bound of the three minima that persist at the highest level of theory used in this study. Because the distance between the ring and the water molecule is 20–30% longer than in (1) or (2), the BSSE is substantially reduced. Figure 4 shows the water–ring distance in (3) to be of the same order as the distance in (2) separating the oxygen in water from the ring hydrogen. Because the computational methods we employed possess an inherent error that may be as large as 1–2 kcal/mol, it is difficult to be certain about the stability of (3). More extensive calculations may conclude that its existence was an artifact of the MP2/aug-cc-pVDZ level of theory.

Adjustments to the electronic binding energy that are required to compute the binding enthalpy, ΔH^{298}, are listed in Table III for conformations (1) and (2). The rotational, translational, and ΔPV terms were taken from the classical expressions, namely, $-1.5RT$, $-1.5RT$, and $-RT$, respectively. Vibrational frequencies based on HF calculations were scaled by 0.893. The final binding enthalpies, combining the best available estimate of the electronic binding energies and the scaled HF/6-31G** thermodynamic contributions, are -6.1, -3.3, and -0.8 kcal/mol for conformations (1), (2), and (3), respectively.

CONCLUSION

Four potential sites for hydrogen bond formation on the phenol–water potential energy surface were examined using extended basis set MP2 calculations. Of these, one minimum disappeared when polarization functions were included to the basis set, two were found to exhibit significant bonds, and the fourth structure displayed a binding energy that was only slightly greater than the inherent uncertainty in the calculations. The strongest of the hydrogen bonds is nearly 3 kcal/mol stronger than the bond in the water dimer, while the weakest is almost 3 kcal/mol weaker.

Structures were determined at three levels of theory, up to and including MP2 with polarized basis sets. The use of HF/3-21G geometries in conjunction with larger basis set, correlated methods to compute energy differences was found to yield binding energies that were slightly more than 1 kcal/mol smaller than values obtained from the better levels of theory. For complexes containing multiple waters, it may be acceptable to limit the geometry optimization to the HF/3-21G level, followed by HF/6-31G** calculations (with no CP correction) to determine the energetics, a procedure similar to that followed by Schütz et al. in their work on phenol + one water. This approach implicitly relies on the fortuitous cancellation of errors that are on the order of 2–3 kcal/mol.

Bond energies were evaluated with diffuse function augmented sets. An estimate of the effect of including multiple ds and fs in the basis set was made on a smaller, prototype system and found to be small. As was the case in the water dimer, the use of the counterpoise correction led to larger changes in binding energies with increasing basis set size than was otherwise observed. Thus, the CP-corrected results were in poorer agreement with the estimated complete basis set limit.

References

1. O. Matsuoka, E. Clementi, and M. Yoshimine, *J. Chem. Phys.*, **64**, 1351 (1976); U. Niesar, G. Corongiu, M. Huang, M. Dupuis, and E. Clementi, *Int. J. Quantum Chem. Symp.*, **23**, 421 (1989); *Modern Techniques in Computational Chemistry: MOTECC-89*, E. Clementi, Ed., ESCON, 1989.

2. J. Caldwell, L.X. Dang, and P.A. Kollman, *J. Am. Chem. Soc.*, **112**, 9144 (1990); L.X. Dang, J.E. Rice, J. Caldwell, and P.A. Kollman, *J. Am. Chem. Soc.*, **113**, 2481 (1991); L.X. Dang, *J. Chem. Phys.*, **96**, 6970 (1992).

3. D. Feller, *J. Chem. Phys.*, **96**, 6104 (1992).

4. J.A. Pople, M. Head-Gordon, and K. Raghavachari, *J. Chem. Phys.*, **90**, 4635 (1989); K. Raghavachari, G.W. Tucks, J.A. Pople, and M. Head-Gordon, *Chem. Phys. Lett.*, **157**, 479 (1989).

5. R.J. Stanley and A.W. Castleman Jr., *J. Chem. Phys.*, **94**, 7744 (1991).

6. T. Ebata, M. Furukawa, T. Suzuki, and M. Ito, *J. Opt. Soc. Am. B*, **7**, 1890 (1990).

7. M. Schütz, T. Bürgi, and S. Leutwyler, *J. Mol. Struct.* (*THEOCHEM*), to appear.

8. J.S. Binkley, J.A. Pople, and W.J. Hehre, *J. Am. Chem. Soc.*, **102**, 939 (1980).

9. W.J. Hehre, R. Ditchfiled, and J.A. Pople, *J. Chem. Phys.*, **56**, 2257 (1972); P.C. Hariharan and J.A. Pople, *Theor. Chim. Acta*, **28**, 213 (1973).

10. M.J. Frisch, J.E. Del Bene, J.S. Binkley, and H.F. Schaefer III, *J. Chem. Phys.*, **84**, 2279 (1986).

11. R. Krishnam, J.S. Binkley, R. Seeger, and J.A. Pople, *J. Chem. Phys.*, **72**, 650 (1980); T. Clark, J. Chandrasekhar, and P.V.R. Schleyer, *J. Comp. Chem.*, **4**, 294 (1983).

12. M.J. Frisch, M. Head-Gordon, G.W. Tucks, J.B. Forseman, H.B. Schlegel, K. Raghavachari, M. Robb, J.S.

Binkley, C. Gonzalez, D.J. Defrees, D.J. Fox, R.A. Whitehead, R. Seeger, C.F. Melius, J. Baker, R.L. Martin, L.R. Kahn, J.J.P. Stewart, S. Topiol, and J.A. Pople, Gaussian 90, revision G, Gaussian, Inc., Pittsburgh, PA, 1990.

13. J. Almlof, K. Fraegri, M. Feyereisen, and K. Korsell, DISCO, a direct SCF and MP2 program, 1992.

14. cc-pVDZ through cc-pVQZ: T.H. Dunning Jr., *J. Chem. Phys.*, **90**, 1007 (1989).

15. R.A. Kendall, T.H. Dunning Jr., and R.J. Harrison, *J. Chem. Phys.*, **96**, 6796 (1992).

16. W.S. Benedict, N. Gailar, and E.K. Pyler, *J. Chem. Phys.*, **24**, 1139 (1956).

17. T. Pedersen, N.W. Larsen, and L. Nygaard, *J. Mol. Struct.*, **4**, 59 (1969).

18. The experimental water geometry is taken from J.H. Callomon, E. Hirota, T. Iijima, K. Kichitsu, W.J. Lafferty, Lanolt-Bornstein, Springer-Verlag, Berlin, 1987; the experimental phenol geometry is taken from T. Pedersen, N.W. Larsen, and L. Nygaard, *J. Mol. Struct.*, **4**, 59 (1969).

19. W.J. Hehre, L. Radom, P.v.R. Schleyer, and J.A. Pople, *Ab Initio Molecular Orbital Theory*, John Wiley & Sons, New York, 1986.

20. G. Strey, *J. Mol. Spectrosc.*, **24**, 87 (1967).

21. S.L. Anderson, L. Goodman, K. Krogh-Jespersen, A.G. Ozkabak, R.N. Zare, and C. Zheng, *J. Chem. Phys.*, **82**, 5329 (1985).

22. H.D. Bist, J.C.D. Brand, and D.R. Williams, *J. Mol. Spectrosc.*, **24**, 402 (1967).

23. J.A. Pople, M. Head-Gordon, D.J. Fox, K. Raghavachari, and L.A. Curtiss, *J. Chem. Phys.*, **90**, 5622 (1989).

24. S.F. Boys and F. Bernardi, *Mol. Phys.*, **19**, 553 (1970).

25. J.E. Del Bene, *Int. J. Quantum Chem.*, to appear.